GEF-H1 is necessary for neutrophil shear stress–induced migration during inflammation

Noah Fine,[1,2,3]* Ioannis D. Dimitriou,[1,4]* Jacob Rullo,[6] María José Sandí,[1] Björn Petri,[7] Jack Haitsma,[8] Hisham Ibrahim,[6] Jose La Rose,[1] Michael Glogauer,[3] Paul Kubes,[7] Myron Cybulsky,[6] and Robert Rottapel[1,2,4,5,6]

[1]Princess Margaret Cancer Center, Toronto, Ontario M5G 1L7, Canada
[2]Department of Medical Biophysics, University of Toronto, Toronto, Ontario M5S 1L7, Canada
[3]Matrix Dynamics Group, University of Toronto, Toronto, Ontario M5S 3E2, Canada
[4]Department of Immunology and [5]Department of Medicine, University of Toronto, Toronto, Ontario M5S 1L7, Canada
[6]Toronto General Research Institute, University Health Network, Toronto, Ontario M5G 2C4, Canada
[7]Immunology Research Group, Department of Physiology and Pharmacology, Calvin, Phoebe and Joan Snyder Institute for Infection, Immunity and Inflammation, University of Calgary, Calgary, Alberta T2N 4N1, Canada
[8]Department of Anesthesiology, VU Medical Center, 1081 HV Amsterdam, Netherlands

Leukocyte crawling and transendothelial migration (TEM) are potentiated by shear stress caused by blood flow. The mechanism that couples shear stress to migration has not been fully elucidated. We found that mice lacking GEF-H1 (GEF-H1$^{-/-}$), a RhoA-specific guanine nucleotide exchange factor (GEF), displayed limited migration and recruitment of neutrophils into inflamed tissues. GEF-H1$^{-/-}$ leukocytes were deficient in in vivo crawling and TEM in the postcapillary venules. We demonstrated that although GEF-H1 deficiency had little impact on the migratory properties of neutrophils under static conditions, shear stress triggered GEF-H1–dependent spreading and crawling of neutrophils and relocalization of GEF-H1 to flotillin-2–rich uropods. Our results identify GEF-H1 as a component of the shear stress response machinery in neutrophils required for a fully competent immune response to bacterial infection.

Introduction

Neutrophils are a critical component of the innate immune system and are among the first responders to infection (Borregaard, 2010). Mobilization of neutrophils from the circulation into sites of infection depends on their recruitment to the activated endothelial surface and their ability to crawl and to undergo transendothelial migration (TEM). These events depend on dynamic regulation of integrin-based adhesion receptors and the microtubule (MT) and actin cytoskeletons. During recruitment, neutrophils integrate stimuli from multiple inputs on the endothelial surface, including selectins, integrin ligands, and chemokines. Furthermore, neutrophils and other leukocytes crawl and transmigrate optimally in the presence of shear stress under conditions of blood flow (Alon and Dustin, 2007; Alon and Ley, 2008). Transmigration of neutrophils across activated human umbilical vein endothelial cells (HUVECs) is accelerated in a shear-dependent manner and correlates with the magnitude of shear (Kitayama et al., 2000). Shear stress also promotes neutrophil invagination into the apical endothelial interface (Cinamon et al., 2004). Failure of neutrophils to respond to shear stress can lead to profound clinical immunodeficiency in humans with leukocyte adhesion disorder type 1 (Alon et al., 2003), emphasizing the importance of the shear stress response in normal immune function. Despite being an essential aspect of the leukocyte recruitment cascade, the mechanism that translates shear stress to functionally relevant cellular responses in neutrophils is not well understood.

Cell crawling depends on cell polarity and the forces of adhesion, propulsion, and retraction. These are regulated by Rho family small GTPases (Raftopoulou and Hall, 2004). In leukocytes, RhoA controls contractility in the uropod to maintain cellular polarity and promote migration (Xu et al., 2003). GEF-H1 is a MT-associated RhoA-specific guanine nucleotide exchange factor (GEF; Ren et al., 1998) that couples MT depolymerization with Rho-mediated actin stress fiber formation and cell contraction (Krendel et al., 2002; Chang et al., 2008) and has been implicated in migration of fibroblast (Nalbant et al., 2009), epithelial cells (Tsapara et al., 2010), and T cells (Heasman et al., 2010).

We investigated GEF-H1 function in the neutrophil response after acute bacterial infection and found that GEF-H1$^{-/-}$ neutrophils are intrinsically defective in TEM into sites of inflammation. We further identified a severe crawling and TEM defect in GEF-H1–deficient neutrophils using intravital

*N. Fine and I.D. Dimitriou contributed equally to this paper.

Correspondence to Robert Rottapel: rottapel@uhnresearch.ca

Abbreviations used: CFSE, carboxyfluorescein succinimidyl ester; CLP, cecal ligation and puncture; fMLP, *N*-formyl-methionyl-leucyl-phenylalanine; GEF, guanine nucleotide exchange factor; GPCR, G protein–coupled receptor; HUVEC, human umbilical vein endothelial cell; MFI, mean fluorescence intensity; MT, microtubule; pMLC, phosphorylated myosin light chain; ROCK, Rho-associated protein kinase; TEM, transendothelial migration; TGA, thioglycolate.

The Rockefeller University Press $30.00
J. Cell Biol. Vol. 215 No. 1 107–119
www.jcb.org/cgi/doi/10.1083/jcb.201603109

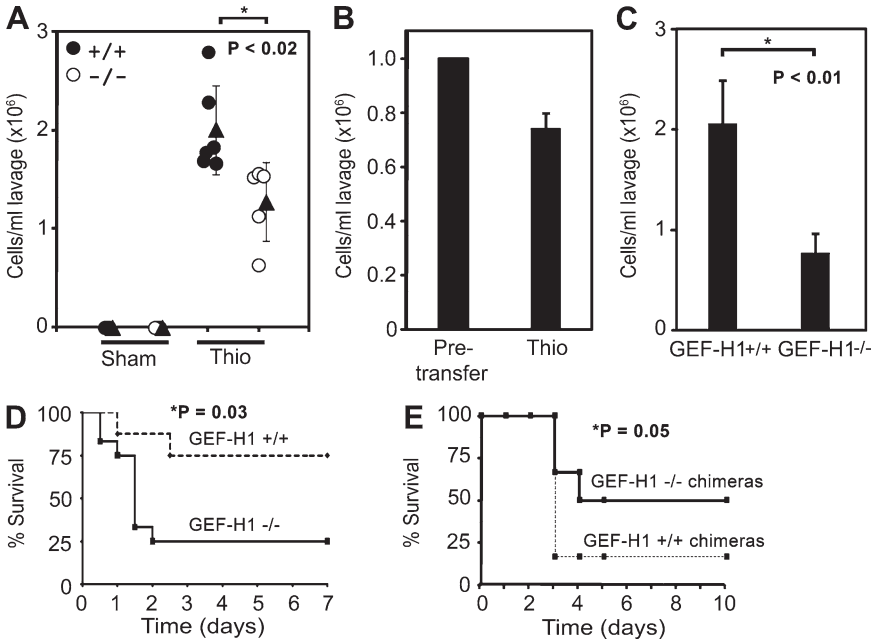

Figure 1. **Neutrophil migration during inflammation and sepsis is defective in GEF-H1$^{-/-}$ mice.** (A) Mice underwent sham (n = 3) or received an intraperitoneal injection of 3% TGA (GEF-H1$^{+/+}$, n = 6; GEF-H1$^{-/-}$, n = 5), and neutrophil yields in the peritoneum were determined 5 h later. Mean values ± SEM are shown. (B) Bone marrow–derived neutrophils were isolated from GEF-H1$^{+/+}$ and GEF-H1$^{-/-}$ mice and transferred by tail vein injection into wild-type recipient mice. Thioglycolate peritonitis (Thio) was induced at the time of neutrophil transfer, and the peritoneum was lavaged 5 h after injection. Ratios of CFSE^{hi} GEF-H1$^{-/-}$ donor cells to CFSE^{lo} GEF-H1$^{+/+}$ donor cells were determined (n = 5) and normalized to pre-transfer ratios. Data are shown as mean ± SEM. (C) Mice underwent CLP-induced sepsis, and the peritoneum was lavaged 12 h after. Mean neutrophil yields are shown ± SEM. (D) GEF-H1$^{+/+}$ (n = 8) and GEF-H1$^{-/-}$ (n = 12) mice underwent CLP surgery, and survival was monitored every 12 h for 1 wk. A p-value was determined using the log-rank Mantel–Cox test. (E) Hematopoietically reconstituted mice were generated as described in Materials and methods. 12 wk after reconstitution, GEF-H1$^{+/+}$ (n = 6) and GEF-H1$^{-/-}$ (n = 6) chimeric mice underwent CLP surgery, and survival was monitored every 12 h for 10 d. A p-value was determined using the log-rank Mantel–Cox test.

microscopy. We examined neutrophil chemokinesis in vitro and found that GEF-H1 is required for directional migration only under shear stress conditions and that shearing forces specifically induced cell spreading and crawling. Lastly, we demonstrated that shear stress triggers GEF-H1 dephosphorylation and relocalization from the MT array to the uropod. Together, these findings show that GEF-H1 is required to couple intravascular shear stress with Rho-dependent migratory behavior of neutrophils during inflammation.

Results

GEF-H1 is required for efficient in vivo neutrophil recruitment during inflammation

Neutrophils are the primary antibacterial responders in the first hours of infection (Borregaard, 2010). We therefore examined the competency of neutrophils to migrate into the peritoneum of GEF-H1$^{+/+}$ and GEF-H1$^{-/-}$ mice after thioglycolate (TGA)–induced peritonitis. Complete blood count and differential analysis confirmed that red blood cell, granulocyte, and platelet numbers were not reduced in GEF-H1–deficient mice (Fig. S1); however, recruitment of neutrophils into the peritoneum in response to sterile inflammation was impaired in GEF-H1$^{-/-}$ mice compared with wild-type controls (Fig. 1 A). To determine if there is a cell-autonomous migration defect in GEF-H1$^{-/-}$ neutrophils, we performed a competitive adoptive transfer experiment where differentially carboxyfluorescein succinimidyl ester (CFSE)–labeled wild-type and GEF-H1$^{-/-}$ neutrophils were mixed in equal proportions and transferred into a syngeneic wild-type host mouse by tail vein injection followed by chemically induced peritonitis. We found that the recruitment of wild-type neutrophils into the peritoneum consistently outcompeted the knockout neutrophils (Fig. 1 B). The decreased ratio of GEF-H1$^{-/-}$ neutrophils relative to GEF-H1$^{+/+}$ neutrophils that were recruited recapitulated the relative defect in TGA-induced recruitment of neutrophils in GEF-H1$^{-/-}$ mice (Fig. 1 B).

To further assess the migratory defect of neutrophils lacking GEF-H1, we used a mouse model of cecal ligation and puncture (CLP)–induced microbial sepsis. Similar to the findings using TGA, the number of neutrophils infiltrating the peritoneum 12 h after CLP-induced sepsis is significantly reduced in GEF-H1$^{-/-}$ mice compared with wild-type controls (Fig. 1 C), a result that further underscores the role of GEF-H1 in regulating neutrophil migration. Interestingly, although inhibition of neutrophil infiltration has been associated with increased survival in septic animal (Lerman et al., 2014), we observed a survival defect in GEF-H1$^{-/-}$ mice, the majority of which died within 48 h of surgery (Fig. 1 D). This observation indicated that GEF-H1 deficiency likely affects other cell populations in addition to neutrophils that determine the host response to bacterial infection.

Many of the inflammatory mediators of sepsis can induce endothelial barrier dysfunction, which in turn increases vascular permeability and leads to an exaggerated inflammatory response with associated tissue damage and subsequent organ dysfunction (Eisa-Beygi and Wen, 2015). GEF-H1 localizes to tight junctions in epithelial and endothelial cells, where it potentiates paracellular permeability (Benais-Pont et al., 2003; Kakiashvili et al., 2009; Birukova et al., 2010). We used intravital microscopy to measure the integrity of the microvasculature in GEF-H1$^{+/+}$ and GEF-H1$^{-/-}$ mice after superfusion with *N*-formyl-methionyl-leucyl-phenylalanine (*f*MLP). Leakage of a fluorescently labeled albumin tracer from the vasculature into the extravascular space was monitored in normal and neutrophil-depleted GEF-H1$^{+/+}$ and GEF-H1$^{-/-}$ mice. Upon superfusion, similar increases in vascular permeability index were observed in GEF-H1$^{+/+}$ and GEF-H1$^{-/-}$ mice (Fig. S2). When neutrophils were depleted, the vasculature of GEF-H1$^{+/+}$ mice was impermeable to the fluorescently labeled tracer. In contrast, the vasculature of GEF-H1$^{-/-}$ mice demonstrated significant permeability after neutrophil depletion as indicated by an increase in the permeability index after *f*MLP superfusion. Permeability of the GEF-H1$^{-/-}$ vasculature was similar regardless

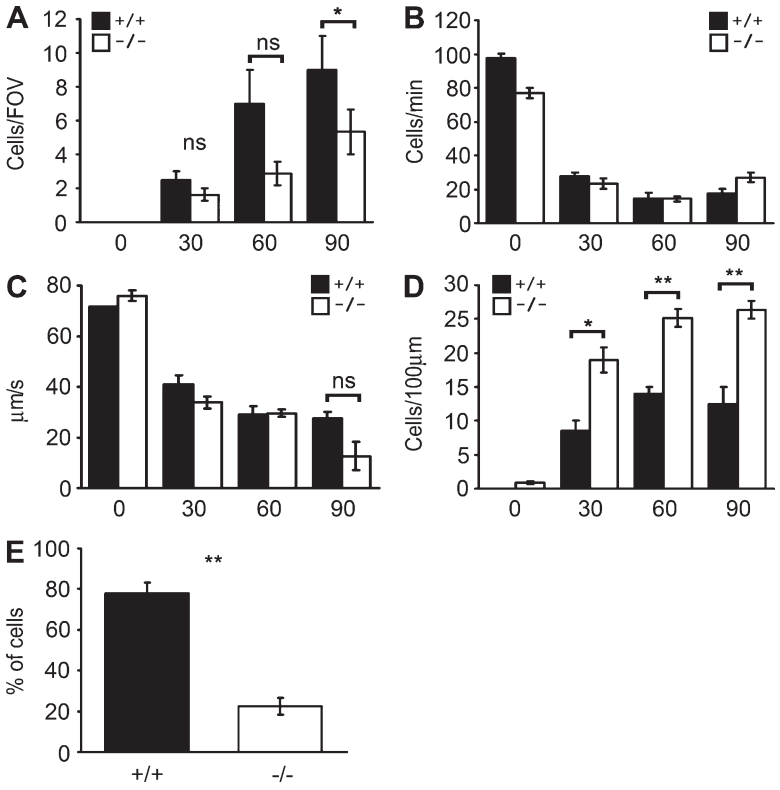

Figure 2. **In vivo leukocyte recruitment was monitored upon superfusion of the exposed mouse cremaster with *f*MLP.** (A) Emigration was determined from the total number of cells observed in the extravascular space adjacent to the observed venule within the microscopic field of view (FOV). (B) Rolling flux was measured as the number of rolling leukocytes that pass through a 100-µm section of vessel per minute. (C) Rolling velocity was calculated from the time required for a cell to roll along a 100-µm length of vessel and is expressed as micrometers per second. (D) Cell accumulation was quantified as the number of adherent cells within a 100-µm length of venule in 5 min. A cell was deemed adherent if it remained stationary for at least 30 s. (E) The percentage of crawling cells was determined from the number of adherent cells that showed a clear crawling behavior. Data are presented as mean ± SD values from three GEF-H1$^{+/+}$ and three GEF-H1$^{-/-}$ mice. ANOVA with Bonferroni's correction was performed to determine p-values (ns, not significant; *, $P < 0.05$; **, $P < 0.001$).

of whether neutrophils were depleted or not, suggesting that GEF-H1 is required to limit endothelial permeability. In GEF-H1–deficient mice, a defective endothelial barrier may account for the increased mortality during sepsis despite the inability of GEF-H1$^{-/-}$ neutrophils to migrate into the inflammation site.

We generated chimeric mice by hematopoietic reconstitution to directly assess the role of GEF-H1 in neutrophil migration after sepsis. We hypothesized that the inability of GEF-H1–deficient neutrophils to efficiently migrate through the intact endothelium would protect from the severe tissue damage induced by sepsis. Wild-type mice were lethally irradiated and reconstituted with bone marrow from either GEF-H1$^{+/+}$ or GEF-H1$^{-/-}$ mice. Complete reconstitution was confirmed 10 wk later by flow cytometry (Fig. S3). As shown in Fig. 1 E, we observed an increased survival in GEF-H1$^{-/-}$ chimeric mice compared with the control group after CLP-induced sepsis, which demonstrates the protective role of neutrophil migratory deficiency in sepsis lethality.

The ability to roll, adhere, and crawl on the inflamed endothelium and subsequently undergo TEM is critical for circulating leukocytes to migrate to sites of infection (Springer, 1994). To ascertain which steps in the recruitment cascade are compromised in GEF-H1–deficient neutrophils, we visualized the real-time behavior of neutrophils in the cremasteric muscle capillaries after superfusion with *f*MLP by intravital microscopy. 90 min after superfusion, we observed defective accumulation of leukocytes in the extravascular space in GEF-H1$^{-/-}$ mice relative to GEF-H1$^{+/+}$ mice (Fig. 2 A). The rolling flux and the velocity of rolling leukocytes in GEF-H1$^{+/+}$ and GEF-H1$^{-/-}$ mice were similar (Fig. 2, B and C). Adherent leukocytes began to accumulate on the vascular surface after superfusion; however, at all time points, there was a greater accumulation of GEF-H1$^{-/-}$ leukocytes compared with GEF-H1$^{+/+}$ leukocytes (Fig. 2 D). We also observed a 70% reduction in the proportion of adherent GEF-H1$^{-/-}$ cells that crawled compared with GEF-H1$^{+/+}$ cells (Fig. 2 E). Hence, GEF-H1$^{-/-}$ leukocytes accumulate on the endothelial surface as a result of defective crawling and TEM in vivo.

In vitro adhesion and migration is normal in GEF-H1$^{-/-}$ neutrophils

To recapitulate the defective migration of GEF-H1$^{-/-}$ leukocytes observed in the mouse vasculature, we analyzed in vitro adhesion and migration of primary bone marrow–derived neutrophils from GEF-H1$^{+/+}$ and GEF-H1$^{-/-}$ mice. First, we tested adhesion of fluorescently labeled neutrophils added to a confluent monolayer of HUVECs in the presence of DMSO or *f*MLP. Based on recovery of fluorescence intensity, *f*MLP induced a twofold increase in mean neutrophil adhesion compared with DMSO-treated cells (Fig. 3 A). There was no difference between adhesion of GEF-H1$^{+/+}$ and GEF-H1$^{-/-}$ neutrophils under unstimulated or *f*MLP-stimulated conditions.

Next, we tested the ability of neutrophils to migrate across a confluent HUVEC monolayer in response to *f*MLP using a transwell system. We observed no difference in the ability of GEF-H1$^{+/+}$ and GEF-H1$^{-/-}$ neutrophils to transmigrate across the endothelial barrier (Fig. 3 B).

We tested the ability of neutrophils to migrate in a 3D-collagen matrix toward a C5a gradient (Fig. 3 C and Fig. S4, A–D). Cells were monitored by time-lapse video microscopy, and individual cell trajectories were determined. Cell migration parameters were determined from analysis of cell trajectory plots. We observed that both GEF-H1$^{+/+}$ and GEF-H1$^{-/-}$ neutrophils chemotax equally under these conditions.

Shear stress–induced crawling is defective in GEF-H1$^{-/-}$ neutrophils

To assess migration of neutrophils in response to physiological ligands, cells were monitored on ICAM-1–coated surfaces in

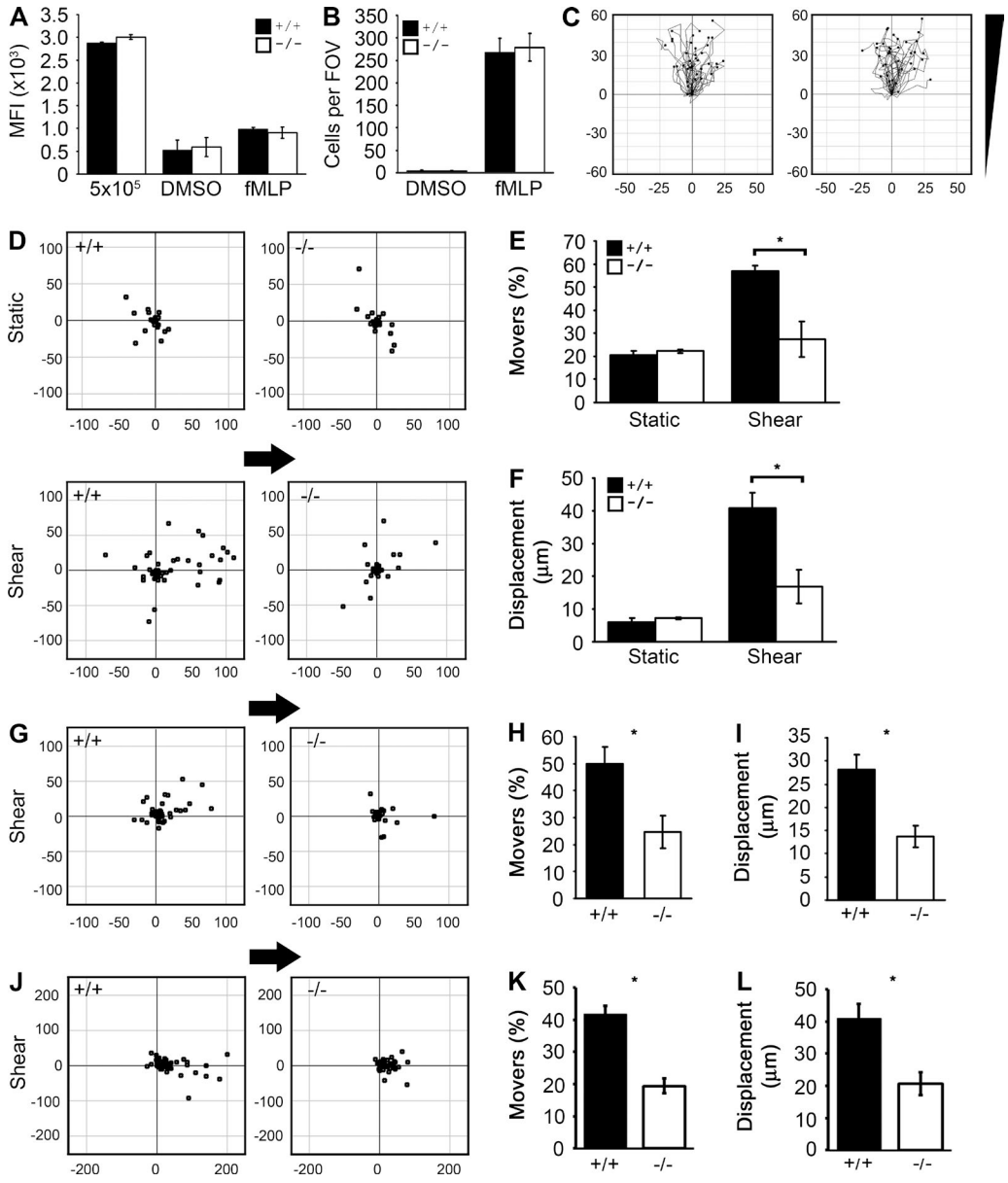

Figure 3. **GEF-H1 is specifically required for shear stress–induced neutrophil migration.** (A) Fluorescently labeled GEF-H1$^{+/+}$ and GEF-H1$^{-/-}$ neutrophils (5×10^5) were plated on HUVECs in triplicate and treated with *f*MLP or DMSO. Nonadhered cells were removed, and mean fluorescence intensity (MFI) per well was determined. MFI of labeled neutrophils is shown as a positive control. Shown are means ± SD. (B) Fluorescently labeled neutrophils were plated in triplicate on confluent HUVECs in transwell filters. Cells were allowed to transmigrate for 1 h toward 1 µM *f*MLP in the wells below each filter. Transmigrated cells were imaged at 20× by widefield microscopy, and automated cell counting was performed using CellProfiler software. Three independent experiments were performed. Results are mean ± SD from a representative experiment. FOV, field of view. (C) GEF-H1$^{+/+}$ and GEF-H1$^{-/-}$ neutrophils were resuspended in a collagen matrix, and migration toward a gradient of C5a was monitored in triplicate wells. Representative data from one experiment are shown. Distance from the origin is indicated on x and y axes in µm. The direction of the chemotactic gradient is indicated. (D–L) GEF-H1$^{+/+}$ and GEF-H1$^{-/-}$ neutrophils were stimulated with *f*MLP and plated on ICAM-1–coated surfaces (D–F), TNF-activated HUVECs (G–I), or TNF-activated C166 mouse endothelial cells (J–L). Cell migration in the presence or absence of 4 dynes/cm^2 constant shear stress was determined from at least 60 cells per experiment. Mean percentage of migrating cells (E, H, and K) and the mean cell displacement (F, I, and L) ± SEM are indicated and were determined from three independent experiments. Moving cells were defined as those that migrated a minimum distance of 15 µm. Neutrophil positions relative to the origin are indicated from a representative experiment (D, G, and J). Distance from the origin is indicated on the x and y axes in micrometers. Arrows indicate direction of shear.

the presence of *f*MLP (Fig. 3, D–F). Approximately 20–25% of adherent neutrophils exhibited random chemokinetic crawling, with a mean displacement during this time frame of ∼7 µm. There was no difference in the crawling behavior of GEF-H1$^{+/+}$ and GEF-H1$^{-/-}$ neutrophils.

Intravascular shear stress is a potent trigger for leukocyte crawling on activated endothelia (Kitayama et al., 2000). We therefore analyzed the migratory behavior of GEF-H1–deficient neutrophils under conditions of shear stress. Neutrophils were adhered to TNF-activated HUVECs, TNF-activated C166 mouse endothelial cells, or ICAM-1–coated surfaces in the presence of *f*MLP. After settling for 5 min, cells were monitored during exposure to 4 dynes/cm^2 shear stress. Cell displacement, determined by video microscopy, indicated that the majority of motile cells migrated in the direction of flow (Fig. 3, D, G, and J). On ICAM-1–coated surfaces, shear stress

induced an almost threefold increase in the percentage of migratory GEF-H1$^{+/+}$ neutrophils compared with static conditions ($P = 10^{-4}$; Fig. 3 E) and a sixfold increase in their mean displacement ($P = 2 \times 10^{-3}$; Fig. 3 F). In contrast, there was no increase in the mean percentage of migratory GEF-H1$^{-/-}$ neutrophils or their mean displacement under shear stress. Similar shear-dependent defects of GEF-H1$^{-/-}$ neutrophils were observed on activated HUVECs (Fig. 3, H and I) or activated mouse endothelial cells (Fig. 3, K and L).

Shear stress induces neutrophil spreading in a GEF-H1–dependent manner

Neutrophil crawling in response to shear stress depends on the transition from a rounded morphology to a spread morphology characterized by extension of a lamellipod (Coughlin and Schmid-Schönbein, 2004). We examined whether the defective shear stress induced migratory behavior of GEF-H1$^{-/-}$ neutrophils was correlated to a defect in shear stress–induced cell spreading. We analyzed the spread area of GEF-H1$^{+/+}$ and GEF-H1$^{-/-}$ neutrophils under static and shear stress conditions (Fig. 4, A and B). The cell area frequency distribution showed two populations, representing either rounded or spread cells. GEF-H1$^{+/+}$ neutrophils had a greater mean spread area after exposure to shear stress compared with static conditions. In contrast to wild-type neutrophils, shear stress failed to induce spreading of GEF-H1$^{-/-}$ neutrophils.

To confirm the effects of shear stress we imaged GEF-H1$^{+/+}$ and GEF-H1$^{-/-}$ neutrophil responses at high magnification. Motile cells were seeded and imaged in the absence of shear stress and after exposure to 4 dynes/cm^2 constant shear stress. A representative GEF-H1$^{+/+}$ neutrophil responded immediately to shear stress exposure and transitioned from an amoeboid type of motion to a fully spread morphology within 45 s of shear stress exposure (Fig. 4 C and Video 1). The cell remained spread and motile for the duration of the shear regimen. In contrast, GEF-H1$^{-/-}$ neutrophils failed to spread or crawl in response to shear stress (Video 2).

GEF-H1 exists in MT and non-MT-associated pools in HL-60 cells

Our data suggest that GEF-H1 is required for shear stress–induced spreading and migratory behavior of neutrophils. We next examined the distribution of endogenous GEF-H1 in HL-60 cells under ambient or shear stress conditions by immunofluorescent staining. To track the pool of inactive GEF-H1 in cells, we used an antibody that recognizes the inactive form of GEF-H1 that is phosphorylated at serine 885 (Meiri et al., 2009, 2012; Yamahashi et al., 2011). We found that endogenous GEF-H1 and GEF-H1-pS885 colocalized with MTs in HL-60 cells (Fig. 5 A). A subset of HL-60 cells under static conditions, or after exposure to shear stress, had a discrete pool of cytoplasmic GEF-H1 not associated with MTs that did not stain with the pS885 antibody, indicating that this pool of GEF-H1 was likely in its active state (Fig. 5 B).

GEF-H1 localizes to uropods in response to shear stress

To further characterize the non–MT-associated pool of GEF-H1 we performed immunofluorescent staining with an antibody to flotillin-2, a known uropod-associated protein. We found that the localization of non-MT associated GEF-H1 was highly correlated with flotillin-2, indicating that this pool of GEF-H1

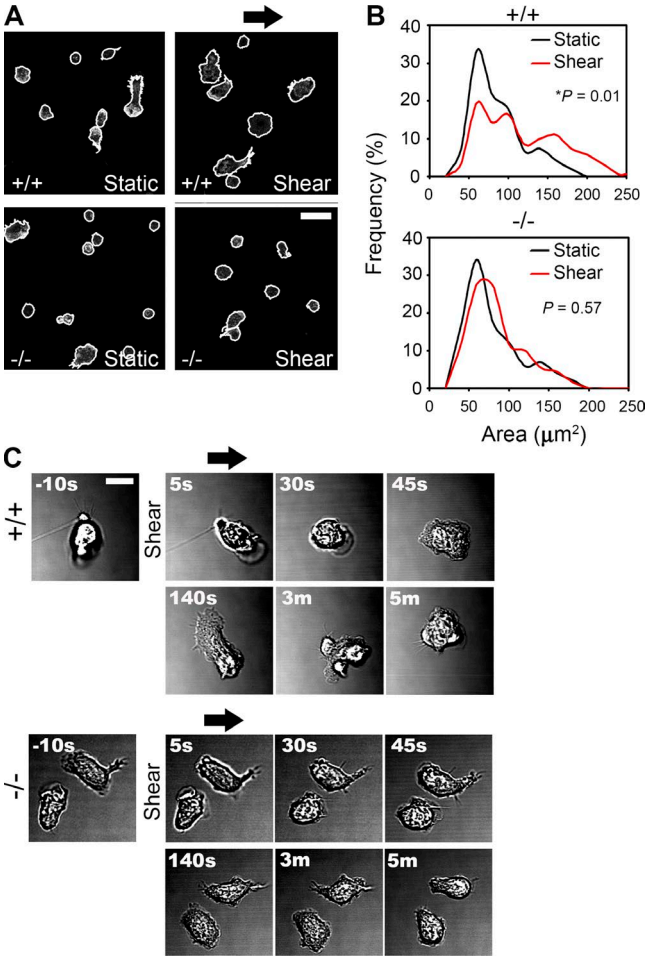

Figure 4. **GEF-H1 is required for shear stress–induced neutrophil spreading.** (A) GEF-H1$^{+/+}$ and GEF-H1$^{-/-}$ neutrophils were stimulated with *f*MLP, plated on ICAM-1–coated coverslips, left untreated or exposed to 4 dynes/cm^2 constant shear stress for 5 min, and then fixed and stained. DAPI images were used to identify primary objects and phalloidin images were subsequently used to determine cell spread areas. Representative images of phalloidin staining are shown with cell outlines overlaid in white. Bar, 20 μm. (B) Frequency distributions showing cell spread areas were derived from observations pooled from three independent experiments. At least 180 cells were measured for each condition. Outliers that were 1.5 times the interquartile range above the third quartile or below the first quartile were removed. Student's *t* test was used to determine p-values by comparing mean spread areas ($n = 3$). (C) Representative high-magnification time course images of individual cell responses to shear stress. Time after induction of shear stress is indicated. Bar, 10 μm. Arrows indicate the direction of shear.

is localized in the uropod (Fig. 5 C). Next, we quantified the fraction of HL-60 cells that exhibited uropod-associated GEF-H1 in static conditions and after exposure to shear stress. After exposure to shear stress, we observed a rapid translocation of GEF-H1 to uropod structures (Fig. 5 D).

MT depolymerization induces GEF-H1–dependent contractility and uropod formation

We emulated the effects of shear stress–induced GEF-H1 activation using the potent MT depolymerizing agent and GEF-H1 activator nocodazole to compare the cell morphological and biochemical responses in GEF-H1$^{+/+}$ and GEF-H1$^{-/-}$ neutrophils (Chang et al., 2008). We assessed the effect of nocodazole

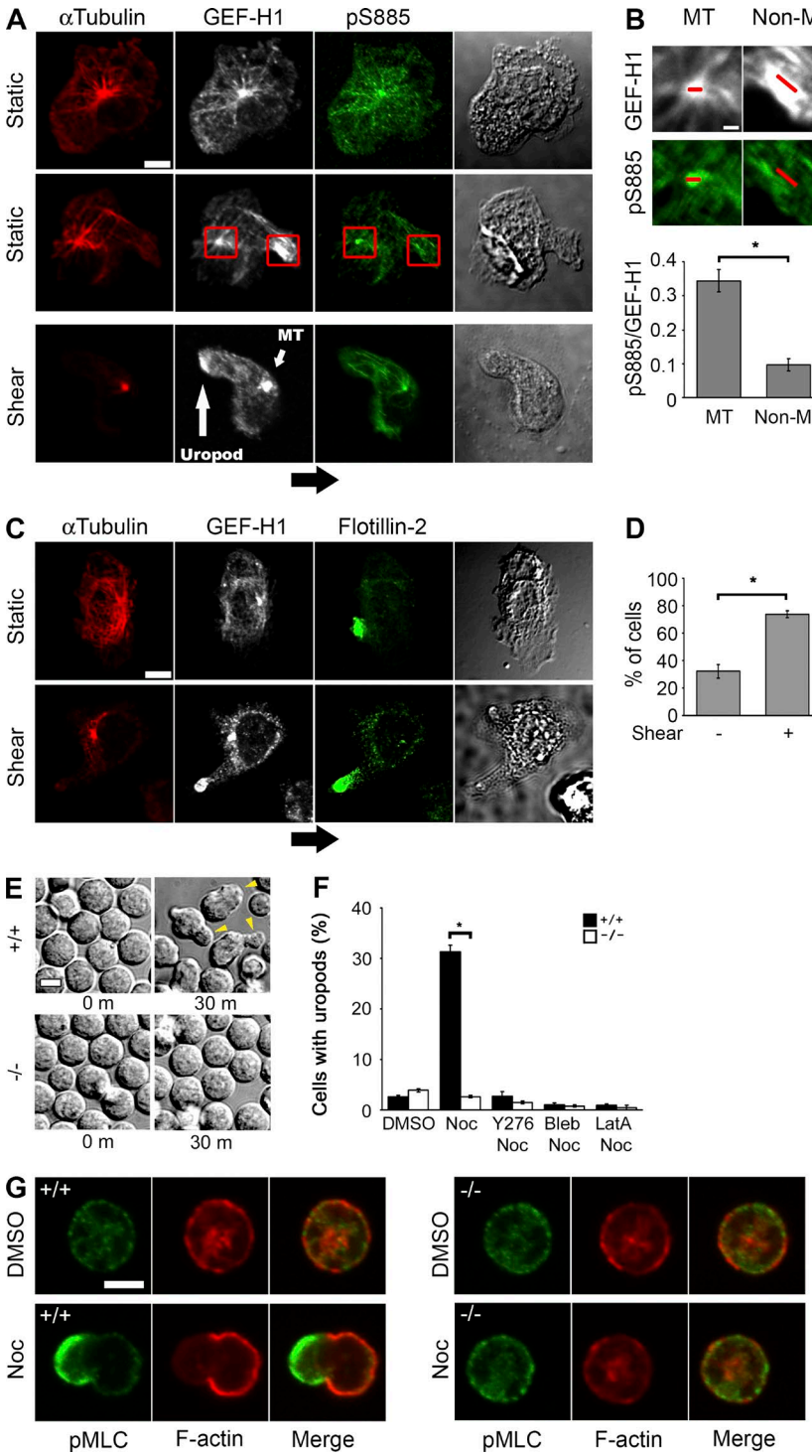

Figure 5. **GEF-H1 relocalizes to uropods immediately after exposure to shear stress.** (A) HL-60 cells were exposed to static or shear stress conditions and were immunolabeled with antitubulin, anti–GEF-H1, or anti–pS885-specific antibodies as indicated. Red boxes highlight MT and non–MT-associated pools of GEF-H1. Bar, 5 µm. (B) A detail from (A) highlighting MT and non–MT-associated pools of GEF-H1. Red bars indicate where the MFIs of pS885 and GEF-H1 were measured. The mean ratio of pS885/GEF-H1 ± SEM was determined from 6–10 random polarized cells in each of five separate experiments. Bar, 1 µm. (C) HL-60 cells were plated on ICAM-coated surfaces and exposed to 2 dynes/cm^2 of shear stress for 20 s or left in shear-free conditions, fixed and stained with the indicated antibodies. Arrow indicates direction of shear. Bar, 5 µm. (D) Localization of GEF-H1 in uropods was determined based on colocalization with flotillin-2. 30 random spread cells were scored per experiment. The means ± SEM of the percentage of cells with uropod-associated GEF-H1 were determined from at least five independent experiments. (E) GEF-H1$^{+/+}$ and GEF-H1$^{-/-}$ neutrophils were imaged at 30 min after stimulation with 10 µM nocodazole by phase-contrast microscopy at 63× magnification. Arrowheads indicate uropods. Bar, 5 µm. (F) Neutrophils were untreated or pretreated for 30 min with 10 µM Y-27632 (Y276), 100 µM blebbistatin (Bleb), or 10 µM latrunculin A (LatA), followed by an additional 30-min incubation with DMSO or 10 µM nocodazole. At least 100 cells were scored per experiment. Data are presented as mean ± SEM and are representative of three independent experiments. (G) Neutrophils were treated with DMSO or nocodazole (Noc) for 30 min and then fixed and labeled for F-actin (red) and pMLC (green). Cells were imaged by confocal fluorescence microscopy at 60× magnification. Bar, 5 µm.

on neutrophil morphology. 3 min after stimulation with nocodazole, GEF-H1$^{+/+}$ neutrophils exhibited dynamic membrane blebbing, which was entirely absent in GEF-H1$^{-/-}$ neutrophils (Fig. S5). By 30 min, many GEF-H1$^{+/+}$ neutrophils were polarized with highly dynamic and contractile uropods (Video 3). In distinction, nocodazole-treated GEF-H1$^{-/-}$ neutrophils lacked the morphological and contractile changes observed in GEF-H1$^{+/+}$ neutrophils (Video 3). After 30 min of stimulation with nocodazole, there was a 10-fold increase in the percentage of GEF-H1$^{+/+}$ neutrophils with uropods but no increase in uropod formation in GEF-H1$^{-/-}$ neutrophils (Fig. 5, E and F). Nocodazole-induced uropod formation was completely blocked by Y-27632, blebbistatin, and latrunculin A, specific inhibitors of the Rho-associated protein kinase (ROCK), myosin activity, and polymerized actin (F-actin), respectively.

To assess nocodazole induced changes in F-actin and phosphorylated myosin light chain (pMLC) in polarized neutrophils, neutrophils were imaged by confocal microscopy. Naive neutrophils had a rounded morphology with F-actin and pMLC preferentially localized at the cortex (Fig. 5 G). After 30 min of stimulation with nocodazole, GEF-H1$^{+/+}$ neutrophils that were polarized displayed mutually exclusive enrichment of pMLC

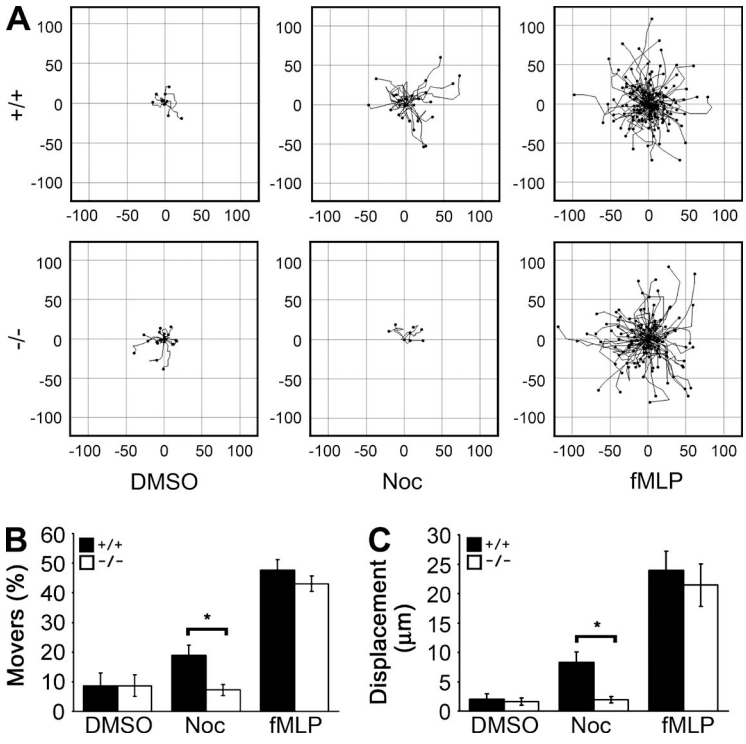

Figure 6. **GEF-H1 is required for MT depolymerization–induced neutrophil polarization and random migration.** (A) GEF-H1$^{+/+}$ and GEF-H1$^{-/-}$ neutrophils were treated with DMSO or nocodazole (Noc) for 30 min or *f*MLP for 5 min, and random migration was monitored for 10 min. Motion tracks from a representative experiment are shown. Distance from the origin is indicated on x and y axes in micrometers. Mean percentage of migrating cells (B) and the mean cell displacement (C) ± SEM are indicated and were determined from three independent experiments. More than 100 cells were tracked per experiment. Moving cells were defined as those that migrated a minimum distance of 15 μm.

and F-actin at the cortex at opposing ends of the cell. GEF-H1$^{-/-}$ neutrophils did not form uropods or display polarization of pMLC and F-actin after treatment with nocodazole.

MT depolymerization induces GEF-H1–dependent chemokinesis

MT depolymerization is known to induce random migration of neutrophils (Niggli, 2003a). We tested the requirement for GEF-H1 in MT depolymerization and chemoattractant-induced neutrophil migration. Neutrophils were treated with DMSO, nocodazole, or *f*MLP, and cells were monitored by time-lapse video microscopy for motion tracking (Fig. 6 A). GEF-H1$^{+/+}$ neutrophils stimulated with nocodazole showed a doubling in the percentage of migrating cells (Fig. 6 B) and a quadrupling of the mean cell displacement (Fig. 6 C) relative to DMSO-treated controls. In contrast, nocodazole failed to stimulate migration of GEF-H1$^{-/-}$ neutrophils. *f*MLP-induced migration of GEF-H1$^{+/+}$ and GEF-H1$^{-/-}$ neutrophils was similar (Fig. 6, A–C).

MT depolymerization induces GEF-H1–dependent actin polymerization and MLC phosphorylation

We analyzed MLC phosphorylation and actin polymerization, two important effector responses of Rho signaling. A flow cytometric approach was used to determine total cellular F-actin in GEF-H1$^{+/+}$ and GEF-H1$^{-/-}$ neutrophils in response to nocodazole (Fig. 7 A). After 2.5 min of nocodazole stimulation, GEF-H1$^{+/+}$ neutrophils displayed a 33% increase in F-actin content compared with DMSO-treated controls, which then decreased gradually over 30 min. In contrast, there was no increase in total F-actin content in GEF-H1$^{-/-}$ neutrophils after treatment with nocodazole. Pretreatment of GEF-H1$^{+/+}$ neutrophils with Y-27632 blocked the increase in pMLC levels and F-actin content, suggesting that ROCK is necessary for nocodazole-induced GEF-H1–dependent actomyosin activation.

MLC phosphorylation was assessed after stimulation of GEF-H1$^{+/+}$ and GEF-H1$^{-/-}$ neutrophils with DMSO, nocodazole, or chemotactic peptide (Fig. 7 B). After 1 min of nocodazole stimulation, GEF-H1$^{+/+}$ neutrophils displayed a pronounced increase in pMLC levels, which peaked at 2.5 min and then decreased gradually over 30 min. In distinction to wild-type neutrophils, nocodazole-induced MLC phosphorylation was absent in GEF-H1$^{-/-}$ neutrophils. Neutrophil stimulation with *f*MLP, CXCL1, or C5a caused robust MLC phosphorylation in GEF-H1$^{+/+}$ and GEF-H1$^{-/-}$ neutrophils (Fig. 7 C), indicating that chemoattractant induction of MLC phosphorylation occurs through a distinct pathway from nocodazole that is independent of GEF-H1. Our data show that neutrophil uropod formation and chemokinesis in response to nocodazole require GEF-H1–dependent stimulation of the Rho signaling axis.

MT depolymerization is not necessary for shear stress–induced GEF-H1 activation

Because GEF-H1 was necessary for neutrophil polarization in response to nocodazole, we determined whether MT depolymerization is necessary for redistribution of GEF-H1 to the uropod in response to shear stress. HL-60 cells were treated with the MT stabilizer Taxol before exposure to shear stress, and the fraction of cells with flotillin-2–associated GEF-H1 was determined (Fig. 8). Taxol-treated HL-60 cells had high levels of polymerized tubulin than untreated controls; however, this did not prevent shear stress–induced relocalization of GEF-H1 to uropods, indicating that this effect is likely to be independent of MT depolymerization.

Discussion

Intravascular shear stress is an essential trigger for recruitment of circulating neutrophils into sites of inflammation. Defects in neutrophil recruitment lead to severe bacterial infections

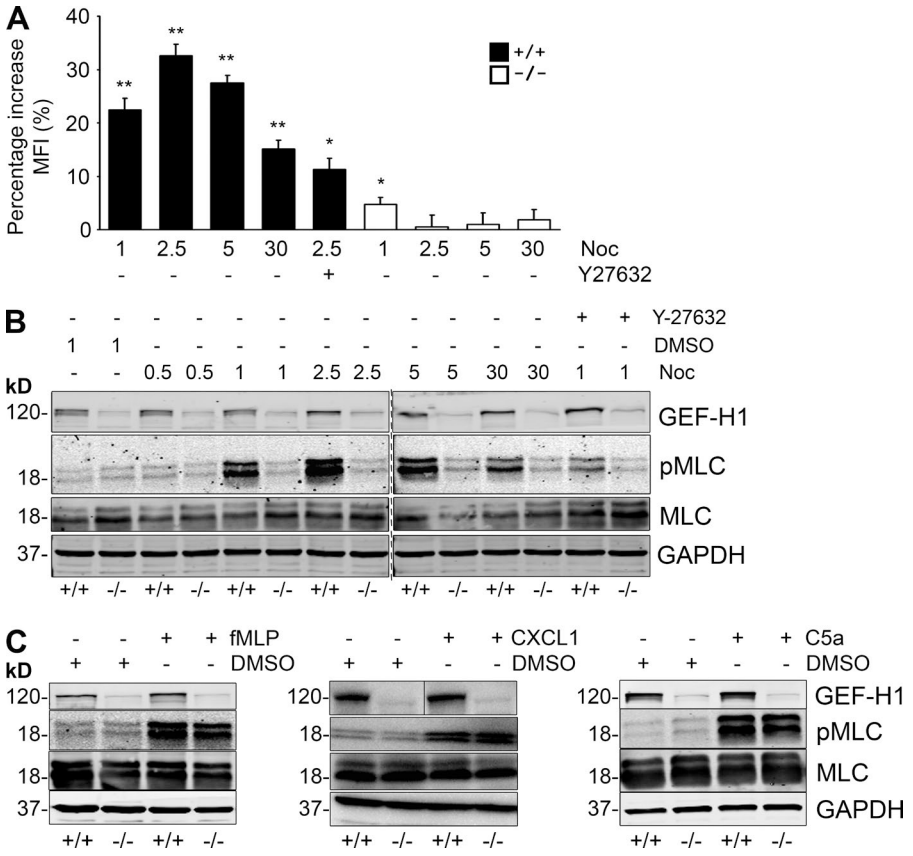

Figure 7. **MT depolymerization induces GEF-H1–dependent actin polymerization and MLC phosphorylation.** (A) GEF-H1$^{+/+}$ and GEF-H1$^{-/-}$ neutrophils were either untreated or pretreated with10 µM Y-27632 for 30 min before stimulation with DMSO or nocodazole (Noc) for the indicated times. The geometric MFI of phalloidin stained cells was determined by flow cytometric analysis of 30,000 gated events in triplicate. Data were pooled from at least four independent experiments, and the mean ± SEM of the percentage increase in F-actin relative to DMSO-treated cells is indicated. (n = 4; *, $P < 0.05$; **, $P < 0.005$). (B) GEF-H1$^{+/+}$ and GEF-H1$^{-/-}$ neutrophils were either untreated or pretreated with 10 µM Y-27632 before stimulation with 10 µM DMSO or nocodazole for the indicated times. Antibodies used for immunoblotting are indicated. Results are combined from two concurrent Western blots, indicated by a dotted line. (C) GEF-H1$^{+/+}$ and GEF-H1$^{-/-}$ neutrophils were treated with 10 µM *f*MLP for 1 min, 10 ng/ml CXCL1 for 5 min, 1 µg/ml C5a for 2 min, or DMSO as a control. Cell lysates were immunoblotted with the indicated antibodies.

and death. We have identified the RhoA-specific GEF, GEF-H1, as a critical regulator of actin polymerization and MLC phosphorylation in neutrophils. In vivo crawling and TEM of GEF-H1–deficient neutrophils are greatly impaired. Although GEF-H1$^{-/-}$ neutrophils are fully able to undergo chemokinesis under basal conditions in vitro, they fail to spread and move purposefully once they are exposed to shear stress, revealing an intrinsic defect in their flow stress transduction machinery. The reduced neutrophil recruitment observed in normal host mice reconstituted with the GEF-H1$^{-/-}$ neutrophils, caused in part by a defective shear stress response, resulted in a significant survival advantage in response to sepsis induction.

GEF-H1 has been implicated in migration of fibroblasts (Nalbant et al., 2009), epithelial cells (Tsapara et al., 2010), and T cells (Heasman et al., 2010). Furthermore, extracellular forces potentiate GEF-H1 activity in pulmonary endothelial cells

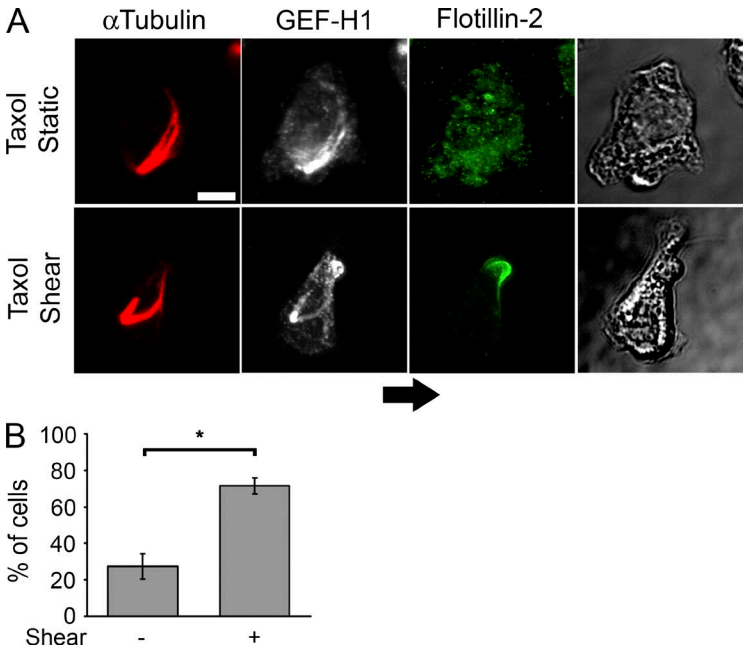

Figure 8. **MT depolymerization is not required for GEF-H1 relocalization in response to shear stress.** (A) HL-60s were incubated for 30 min with 10 µM Taxol and plated on ICAM-coated surfaces. Cells were allowed to settle for 5 min and left in shear-free conditions or exposed to 2 dynes of shear stress. Samples were fixed after 20 s and stained with the indicated antibodies. Arrow indicates direction of shear. Bar, 5 µm. (B) Localization of GEF-H1 in uropods was determined based on colocalization with flotillin-2. 30 random spread cells were scored per experiment. The means ± SEM of the percentage of cells with uropod associated GEF-H1 were determined from at least three independent experiments.

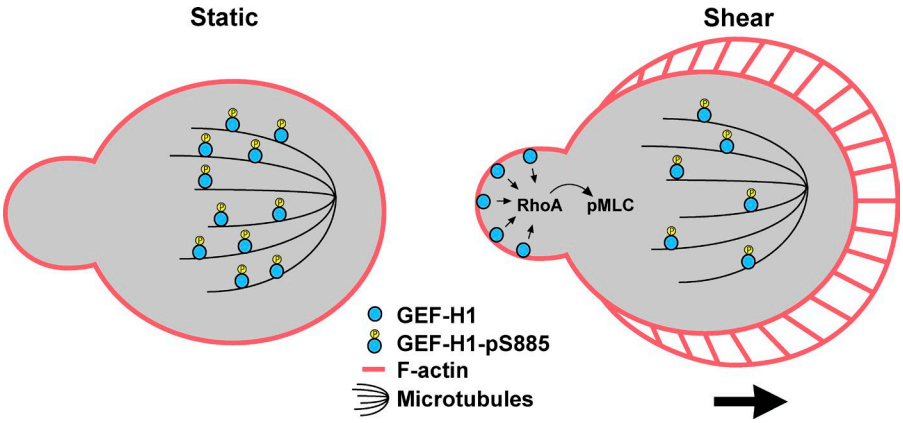

Figure 9. **Model of the GEF-H1–mediated response to shear stress.** Shear stress induces dephosphorylation of GEF-H1 and relocalization from the MT array into the uropod. The dephosphorylated form of GEF-H1 is catalytically active and drives actomyosin-based contraction through Rho-mediated MLC phosphorylation. Although integrins (not depicted) are likely to play an important role in the shear stress response, their role in signaling to GEF-H1 is unclear.

(Birukova et al., 2010) and breast epithelial cells (Heck et al., 2012). GEF-H1 potentiates mechanosensory feedback force on integrins (Guilluy et al., 2011) and relocalizes to integrin-based adhesion complexes in response to intracellular tension (Kuo et al., 2011) in fibroblasts. To uncover the role that GEF-H1 plays in the neutrophil shear stress transduction response, we have shown that GEF-H1 couples to the RhoA–ROCK–pMLC signaling axis required to generate cell contractility and uropods. Uropods in polarized neutrophils are highly contractile structures enriched in adhesion molecules (Alonso-Lebrero et al., 2000; Smith et al., 2007). We have shown that shear stress induces rapid accumulation of GEF-H1 into uropods, where it colocalized with flotillin-2, a uropod-associated component of membrane lipid raft complexes (Rossy et al., 2009). Importantly, we have shown that shear stress induces the dephosphorylated form of GEF-H1, which is catalytically active and accumulates in uropod structures. We conjecture that GEF-H1 increases RhoGTP levels in uropods, which is necessary for neutrophil spreading and crawling through F-actin–dependent integrin function (Laudanna et al., 1996; Anderson et al., 2000) and MLC-dependent contractility (Fig. 9).

Future studies are needed to elucidate how shear stress is coupled to GEF-H1 activation and its relocalization into uropod structures in neutrophils. We have shown that GEF-H1 is dephosphorylated and activated by the PP2A phosphatase (Meiri et al., 2014), suggesting the possibility that PP2A may play a role in shear stress–induced activation of GEF-H1. The mechanotransduction of shear stress is integrated with other costimulatory signals activated by cell surface receptors to optimize cell adhesion, migration, and TEM (Alon and Dustin, 2007; Alon and Ley, 2008). Integrins are likely to play an important role in the shear stress response, because neutrophil exposure to shear stress is a direct consequence of integrin-dependent adhesion on the endothelial surface. Although the role of integrin signaling downstream of shear stress is not known, preliminary results suggest that antibody-mediated clustering of integrins on neutrophils in suspension is not sufficient to induce the dephosphorylation of GEF-H1 at serine 885 (unpublished data). Another receptor system that may contribute to shear stress–induced activation of GEF-H1 could be G protein–coupled receptors (GPCRs). The formylated peptide receptor modulates the shear stress response in neutrophils (Makino et al., 2006), though this pathway does not appear to be coupled to GEF-H1 in our studies. We have demonstrated that GEF-H1 is activated in fibroblasts by the GPCR ligands lysophosphatidic acid or thrombin through stimulation by the $G\alpha_{12/13}$ and $G\beta\gamma$ subunits (Meiri et al., 2014), suggesting that GPCR-mediated activation of GEF-H1 may contribute to shear stress responses in neutrophils. Lastly, shear stress activates ERK in neutrophils (Green et al., 2004), endothelial cells (Sumpio et al., 2005), and stem cells (Yuan et al., 2013). GEF-H1 is a known ERK substrate and is activated by ERK-mediated phosphorylation (Fujishiro et al., 2008), raising the possibility that ERK contributes to shear stress–induced activation of GEF-H1, possibly downstream of integrins (Guilluy et al., 2011). Although nocodazole induces GEF-H1–dependent neutrophil activation, we have shown that GEF-H1 relocalization to uropods in response to shear stress does not require MT depolymerization. This is in contrast to studies using endothelial and epithelial cells, where activation of GEF-H1 by mechanical stress depends on MT depolymerization (Birukova et al., 2010; Heck et al., 2012).

GEF-H1 is a known regulatory component of tight junctions (Benais-Pont et al., 2003). Additionally, shear stress can also alter endothelial cell shape and function (Galbraith et al., 1998; Ji et al., 2008). Our findings differ from RNAi-based studies suggesting that GEF-H1 promotes increased paracellular permeability (Benais-Pont et al., 2003; Kakiashvili et al., 2009; Birukova et al., 2010). We observed increased permeability of the microvasculature in GEF-H1$^{-/-}$ mice, allaying the possibility that defective tight junction integrity could attribute to increased lethality of the GEF-H1–deficient mice. Despite the inability of neutrophils to migrate through the endothelium to the inflammatory site, the increased microvasculature permeability can progressively lead to massive infiltration of inflammatory cells, with subsequent tissue damage and organ failure. Our findings using competitive neutrophil transfer experiments and GEF-H1$^{-/-}$ bone marrow reconstituted wild-type mice indicate that cell-autonomous defects of the GEF-H1$^{-/-}$ neutrophils contribute to decreased peritoneal recruitment independent of endothelial function. However, further studies are necessary to elucidate the functional role of endogenous GEF-H1 in primary endothelial cells.

Here, we provide evidence that GEF-H1 is required for spreading and crawling of neutrophils as part of a mechanosensory response to shear force and thus constitutes a link between mechanosensation and Rho signaling. These results are consistent with the finding that GEF-H1 and its target, RhoA, promote adhesion strengthening and cell stiffening in response to mechanical force in fibroblasts (Guilluy et al., 2011).

A recent study indicates that GEF-H1 is required for macrophage recognition of exogenous nucleic acids and is necessary to establish an effective antiviral response (Chiang et al.,

2014). We show that GEF-H1 performs an additional function within the innate immune response by coupling intravascular shear with the force-sensing machinery in neutrophils to trigger migration into sites of bacterial infection.

Materials and methods

Reagents and antibodies

*f*MLP, blebbistatin, anti–human IgG F(ab')$_2$, and recombinant human TNF were obtained from Sigma-Aldrich. C5a and ICAM-1/Fc chimera were from R&D Systems. Nocodazole and Y-27632 were obtained from EMD Millipore. Latrunculin A was obtained from Alexis Corporation.

Antibodies used for immunoblotting were mouse anti-MLC (1:2,000; Sigma-Aldrich), rabbit anti-pMLC (1:500; Cell Signaling Technology), sheep anti–GEF-H1 (1:500; Exalpha Biologicals), and mouse anti-GAPDH (1:26,000; Sigma-Aldrich).

Antibodies used for immunofluorescent staining were mouse anti–GEF-H1 (1:50; Hycult), rabbit anti–GEF-H1-pS885 (1:200; Cell Signaling Technology), rabbit anti–flotillin-2 (1:100; Santa Cruz Biotechnology, Inc.), rat anti–α-tubulin (1:100; Abcam), and mouse anti-pMLC (1:50; Cell Signaling Technology).

Cells

GEF-H1$^{+/+}$ and GEF-H1$^{-/-}$ mice were generated by targeted gene replacement as described previously (Meiri et al., 2012). The GEF-H1$^{-/-}$ mice have no gross developmental defects. Neutrophils were isolated as previously described (Lowell et al., 1996) and resuspended in Hank's balanced salt solution containing Ca^{2+}/Mg^{2+} (Hanks$^{+/+}$). Preps were ∼80–90% neutrophils based on analysis of the mouse granulocyte marker Gr-1 (BD).

HL-60 cells were obtained from American Type Culture Collection and maintained according to the recommended culture conditions. Cells were differentiated in culture media with 1.4% DMSO as previously described (Makino et al., 2006). HUVECs were maintained in EBM-2 media (Lonza), and the C166 mouse endothelial cell line was maintained in DMEM with 10% FBS. Monolayers were used in experiments 2 d after reaching confluence.

Peritonitis

CLP was performed as previously described (Mei et al., 2010), according to a protocol approved by the Animal Research Committee of the University Health Network. The cecum was ligated and punctured through and through with a 21G needle. Adequate dose of the analgesic Tramadol (20 mg/kg body weight) was given subcutaneously throughout the experiments. For sterile inflammation, 0.5 ml of a 3% TGA solution was administered by intraperitoneal injection. Peritoneal cavities were washed twice with 3 ml cold Hanks$^{-/-}$, and cell counts per milliliter of lavage fluid were determined. Gr-1 positive cells were determined by flow cytometry.

Neutrophil adoptive transfer experiments were performed as previously described (Chen et al., 2012). Bone marrow–derived neutrophils from GEF-H1$^{+/+}$ and GEF-H1$^{-/-}$ mice were labeled with 0.5 µM or 5 µM CFSE for 10 min at room temperature, respectively. This produced differential fluorescent staining of wild-type (low-intensity staining) or knockout neutrophils (high fluorescent staining) that could easily be distinguished by flow cytometry. Labeled cells were mixed in equal ratios (10^7 cells total) and injected through the tail vein into wild-type and GEF-H1$^{-/-}$ syngeneic recipient mice, followed by the induction of thioglycolate chemical peritonitis.

To generate chimeric mice, wild-type recipients (CD45.1$^+$) were lethally irradiated with 9 Gy from a ^{137}cesium source and reconstituted the same day by intravenous injection of 10^7 bone marrow cells, purified using standard methods, from GEF-H1$^{+/+}$ or GEF-H1$^{-/-}$ mice (CD45.2$^+$), respectively. The chimeric mice were monitored after 10 wk for complete reconstitution by flow cytometry and subsequently were subjected to CLP surgery.

Microvascular permeability measurement

Microvascular permeability was quantified based on the degree of vascular albumin leakage from cremasteric venules of GEF-H1$^{+/+}$ and GEF-H1$^{-/-}$ mice, as described previously (Petri et al., 2011). In brief, 25 mg/kg FITC-labeled BSA (Sigma-Aldrich) was administered to the mice intravenously 10 min before each experiment. The exposed cremaster muscle was superfused with 1 µM *f*MLP in warm (37°C) bicarbonate-buffered saline and FITC-derived fluorescence (excitation wavelength, 450–490 nm; emission wavelength, 520 nm) was detected using a spinning disk confocal fluorescent microscope (BX51WI, Olympus) with a 20×/0.95 water XLUMPlan FL objective (Olympus). The microscope was equipped with a confocal light path (WaveFx; Quorum) based on a modified Yokogawa CSU-10 head (Yokogawa Electric Corporation). Image analysis software (ImageJ, 1.44; National Institutes of Health) was used to determine fluorescence intensity in the venule lumen and in the adjacent perivascular tissue. The index of vascular albumin leakage (permeability index) at different time points after *f*MLP superfusion was determined according to the following ratio expressed as a percentage: (mean interstitial intensity − background)/(venular intensity − background). To determine the influence of neutrophil–endothelial interactions on microvascular permeability changes, mice were injected intraperitoneally with 150 µg anti–Gr-1 antibody 24 h before *f*MLP superfusion. This treatment has been shown previously to deplete >95% of mouse neutrophils (Bonder et al., 2004).

Intravital microscopy

Intravital microscopy was performed as previously described (Phillipson et al., 2009). Exposed cremasteric muscle was superfused with 1 µM *f*MLP and visualized with an intravital microscope (Axiolskip; ZEISS) connected to a video camera (5100 HS; Panasonic) using 25× (0.35 N, Fluotar; Leitz) and 40× (0.80 NA, Achroplan; ZEISS) objective lenses. The same five sections of single unbranched cremasteric venules (20–40 µm in diameter) were observed for a given experiment. Adhesion, crawling, and emigration were determined during video playback. Rolling flux and rolling velocity were determined concurrently with intravital analysis of cell adhesion, crawling, and emigration. Rolling leukocytes were defined as those cells moving at a velocity less than that of erythrocytes within a chosen vessel.

Cell migration

Labtek II chambered coverslips (Thermo Fisher Scientific) were used for chemokinesis assays. The center of each well was coated with a 20-µl puddle of 100 µg/ml goat anti–human IgG, blocked with 5% FBS, and then coated with 20 µg/ml Fc-ICAM-1 chimera, each for 1 h at room temperature. Neutrophils were diluted in warm Hanks$^{+/+}$ containing 20 mM Hepes and 1 µM *f*MLP and plated. After 5 min, wells were washed twice, and media containing 1 µM *f*MLP was replaced. Cells were imaged on an inverted microscope (Axiovert 200M; ZEISS) with a heated stage, using a 10× objective (0.5 NA, Fluar; Nikon), a CoolSnap HQ camera (Roper Technologies), and Metamorph software (Molecular Devices). Migration of individual neutrophil was tracked using the manual tracking plugin in ImageJ (National Institutes of Health). Scatterplots and migration parameters were determined using the Chemotaxis and Migration tool (Ibidi).

Shear stress assays were performed as described in the previous paragraph, except that cells were plated on activated HUVECs, acti-

vated C166 cells, or ICAM-1–coated surfaces in a parallel plate flow chamber (Hyduk et al., 2007). Confluent endothelial monolayers were stimulated with 100 ng/ml TNF for 4 h before experiments. Imaging was performed on an inverted phase-contrast microscope (Diaphot 300; Nikon) with a heated stage, connected to a video camera (DXC-151A, Sony) and a video cassette recorder (SVT-S3100; Sony). Neutrophils were infused into the flow chamber and allowed to settle for 5 min. One random field of view was selected, and cell motion was imaged for 10 min after introduction of 4 dynes/cm^2 constant shear stress. Any cells that detached or underwent visible sliding during the course of the experiment were eliminated from the analysis. Cell migration was analyzed as described in the previous paragraph.

Nocodazole and *f*MLP-induced migration was also determined as previously described (Niggli, 2003a,b).

Adhesion assays

Neutrophils were labeled with CellTracker Red (Invitrogen) as per the manufacturer's instructions and resuspended in Hanks$^{+/+}$ with 0.1% BSA, and 5×10^5 cells were plated in triplicate on confluent HUVECs in 96-well plates. Cells were allowed to settle for 10 min at 37°C, 5% CO_2 and supplemented with DMSO or *f*MLP (1 µM final) for an additional 20 min. Plates were spun upside down for 1 min at 100 *g*, and the mean fluorescence intensity (MFI) was determined by spectrofluorometry. As a positive control, 5×10^5 labeled neutrophils were plated in triplicate into empty wells.

Transwell migration assays

Neutrophils were resuspended in Hanks$^{+/+}$ with 0.1% BSA, and 5×10^5 cells were plated in triplicate on top of confluent HUVECs in transwell inserts with a 3 µm pore size (Corning). Inserts were placed in 24-well plates, and cells were allowed to transmigrate for 1 h toward 1 µM *f*MLP or DMSO in the wells below each filter. Inserts were removed and plates were spun for 1 min at 500 *g* to collect transmigrated cells onto 0.1% BSA–coated coverslips at the bottom of each well. Cells were fixed with PFA, and coverslips were mounted on microscope slides in mounting media for further analysis. Phase contrast imaging was performed with a widefield microscope (TE2000-E; Nikon) using a 20× (0.75 NA, Plan Apo; Nikon) objective, an ORCA-ER camera (Hamamatsu Photonics), and Volocity 6.1 software (PerkinElmer). Triplicate wells were imaged for each condition in three independent experiments. Automated cell counting was performed on five random fields of view using CellProfiler software.

3D chemotaxis assay

The 3D chemotaxis assays were performed essentially as described previously (Lämmermann et al., 2008). Neutrophils (1.6×10^6 cells/ml) were resuspended in 1.6 mg/ml PureCol (Advanced Biomatrix) and polymerized in µ-slide VI$^{0.4}$ multichannel slides. Then, 30 µl of C5a (1 µg/ml) was placed in the upper reservoir, and cells were imaged for 30 min. Imaging and analysis were performed as described in the Cell migration section. Moving cells were defined as those that migrated a minimum distance of 15 µm. A directionality of 1 represents straight motion. Cell migration was monitored in triplicate channels in two independent experiments.

Cell spreading

Mouse neutrophils were plated on ICAM-1–coated surfaces under static or shear stress conditions as described in the Cell migration section and fixed with 3.7% PFA. Cells were labeled with phalloidin and DAPI and imaged using a widefield fluorescence microscope (TE2000-E; Nikon) equipped with a 60× oil immersion objective lens (1.4 NA, Plan Apo; Nikon), an ORCA-ER camera (Hamamatsu Photonics), and Volocity 6.1 software (PerkinElmer). CellProfiler software was used for automated determination of cell spread areas.

Immunofluorescence

Primary neutrophils were stimulated at 37°C in suspension for 30 min with DMSO or 10 µM nocodazole and fixed for 20 min with 3.7% PFA. After cytospinning, cells were permeabilized with 0.1% Triton X-100 for 5 min at room temperature and washed with PBS. Samples were then blocked for 1 h with 0.5% BSA and incubated with an anti–pMLC antibody at 4°C overnight. Samples were then incubated with an Oregon Green 488–conjugated anti–mouse IgG and with Texas red–X phalloidin for 30 min at room temperature and mounted. Confocal imaging was performed with an Olympus IX81 inverted confocal microscope using a 60× (1.4 NA, Plan Apo; Nikon) objective and FluoView software (Olympus). Images were acquired with constant microscope sensitivity settings.

Differentiated HL-60 cells were seeded on ICAM-1–coated µ-slide VI$^{0.4}$ multichannel slides (Ibidi). In some experiments, cells were pretreated with Taxol for 30 min. Cells were left untreated or exposed to shear stress for 20 s and fixed for 10 min in ice-cold 100% methanol. Wells were blocked and incubated with primary antibodies and secondary antibodies according to standard protocols. Confocal imaging was performed as described previously.

Uropod assay

Neutrophils were preincubated for 30 min at 37°C in the presence or absence of inhibitors. Cells were then stimulated with nocodazole or DMSO for an additional 30 min, fixed in 1% gluteraldehyde for 20 min at room temperature, and scored for the presence or absence of uropods.

F-actin assay

Neutrophils were either left untreated or pretreated with Y-27632 for 30 min at 37°C before stimulation with nocodazole or DMSO. Cells were fixed with 3.7% paraformaldehyde, permeabilized with 0.1% Triton X-100, and stained with 4 µl Texas Red-X phalloidin for flow cytometric analysis. The percentage increase in F-actin content was expressed relative to DMSO-treated control cells.

Immunoblotting

Neutrophil immunoblots were performed as described previously (Niggli, 2003a,b). Samples were preincubated for 30 min with Y-27632 or buffer before treatment with DMSO, nocodazole, *f*MLP, or C5a.

Statistical analysis

All p-values were determined using a two-way Student's *t* test unless otherwise indicated. Statistical significance was defined as $P < 0.05$ (*).

Online supplemental material

Supplemental material includes data on blood cell counts in GEF-H1$^{-/-}$ mice (Fig. S1), vascular leakage measurements (Fig. S2), data of complete hematopoietic reconstitution after bone marrow transplantation (Fig. S3), neutrophil adhesion and chemotaxis data (Fig. S4), and images of GEF-H1–dependent blebbing of neutrophils (Fig. S5). Additionally, videos of neutrophil responses upon shear stress (Videos 1 and 2) and nocodazole treatment (Video 3) are also included in the supplemental information. Additional data are available in the JCB DataViewer at http://dx.doi.org/10.1083/jcb.201603109.dv.

Acknowledgments

This research was funded by the Canadian Institutes of Health Research. N. Fine was supported by the Natural Sciences and Engineering Research Council of Canada, the Ontario Graduate Scholarship, and the Ontario Graduate Scholarship in Science and Technology (Edward Dunlop Foundation Scholarship).

The authors declare no competing financial interests.

Author contributions: N. Fine, I.D. Dimitriou, and R. Rottapel contributed to the experimental design. N. Fine, J. Rullo, I.D. Dimitriou, M.J. Sandi, B. Petri, J. Haitsma, and H. Ibrahim performed experiments. J. LaRose contributed vital new reagents. M. Glogauer, P. Kubes, and M. Cybulsky contributed vital analytical tools. R. Rottapel, I.D. Dimitriou, and N. Fine wrote the manuscript.

Submitted: 31 March 2016
Accepted: 19 September 2016

References

Alon, R., and M.L. Dustin. 2007. Force as a facilitator of integrin conformational changes during leukocyte arrest on blood vessels and antigen-presenting cells. *Immunity.* 26:17–27. http://dx.doi.org/10.1016/j.immuni.2007.01.002

Alon, R., and K. Ley. 2008. Cells on the run: shear-regulated integrin activation in leukocyte rolling and arrest on endothelial cells. *Curr. Opin. Cell Biol.* 20:525–532. http://dx.doi.org/10.1016/j.ceb.2008.04.003

Alon, R., M. Aker, S. Feigelson, M. Sokolovsky-Eisenberg, D.E. Staunton, G. Cinamon, V. Grabovsky, R. Shamri, and A. Etzioni. 2003. A novel genetic leukocyte adhesion deficiency in subsecond triggering of integrin avidity by endothelial chemokines results in impaired leukocyte arrest on vascular endothelium under shear flow. *Blood.* 101:4437–4445. http://dx.doi.org/10.1182/blood-2002-11-3427

Alonso-Lebrero, J.L., J.M. Serrador, C. Domínguez-Jiménez, O. Barreiro, A. Luque, M.A. del Pozo, K. Snapp, G. Kansas, R. Schwartz-Albiez, H. Furthmayr, et al. 2000. Polarization and interaction of adhesion molecules P-selectin glycoprotein ligand 1 and intercellular adhesion molecule 3 with moesin and ezrin in myeloid cells. *Blood.* 95:2413–2419.

Anderson, S.I., N.A. Hotchin, and G.B. Nash. 2000. Role of the cytoskeleton in rapid activation of CD11b/CD18 function and its subsequent downregulation in neutrophils. *J. Cell Sci.* 113:2737–2745.

Benais-Pont, G., A. Punn, C. Flores-Maldonado, J. Eckert, G. Raposo, T.P. Fleming, M. Cereijido, M.S. Balda, and K. Matter. 2003. Identification of a tight junction-associated guanine nucleotide exchange factor that activates Rho and regulates paracellular permeability. *J. Cell Biol.* 160:729–740. http://dx.doi.org/10.1083/jcb.200211047

Birukova, A.A., P. Fu, J. Xing, B. Yakubov, I. Cokic, and K.G. Birukov. 2010. Mechanotransduction by GEF-H1 as a novel mechanism of ventilator-induced vascular endothelial permeability. *Am. J. Physiol. Lung Cell. Mol. Physiol.* 298:L837–L848. http://dx.doi.org/10.1152/ajplung.00263.2009

Bonder, C.S., M.N. Ajuebor, L.D. Zbytnuik, P. Kubes, and M.G. Swain. 2004. Essential role for neutrophil recruitment to the liver in concanavalin A-induced hepatitis. *J. Immunol.* 172:45–53. http://dx.doi.org/10.4049/jimmunol.172.1.45

Borregaard, N. 2010. Neutrophils, from marrow to microbes. *Immunity.* 33:657–670. http://dx.doi.org/10.1016/j.immuni.2010.11.011

Chang, Y.C., P. Nalbant, J. Birkenfeld, Z.F. Chang, and G.M. Bokoch. 2008. GEF-H1 couples nocodazole-induced microtubule disassembly to cell contractility via RhoA. *Mol. Biol. Cell.* 19:2147–2153. http://dx.doi.org/10.1091/mbc.E07-12-1269

Chen, G., I. Dimitriou, L. Milne, K.S. Lang, P.A. Lang, N. Fine, P.S. Ohashi, P. Kubes, and R. Rottapel. 2012. The 3BP2 adapter protein is required for chemoattractant-mediated neutrophil activation. *J. Immunol.* 189:2138–2150. http://dx.doi.org/10.4049/jimmunol.1103184

Chiang, H.S., Y. Zhao, J.H. Song, S. Liu, N. Wang, C. Terhorst, A.H. Sharpe, M. Basavappa, K.L. Jeffrey, and H.C. Reinecker. 2014. GEF-H1 controls microtubule-dependent sensing of nucleic acids for antiviral host defenses. *Nat. Immunol.* 15:63–71. http://dx.doi.org/10.1038/ni.2766

Cinamon, G., V. Shinder, R. Shamri, and R. Alon. 2004. Chemoattractant signals and beta 2 integrin occupancy at apical endothelial contacts combine with shear stress signals to promote transendothelial neutrophil migration. *J. Immunol.* 173:7282–7291. http://dx.doi.org/10.4049/jimmunol.173.12.7282

Coughlin, M.F., and G.W. Schmid-Schönbein. 2004. Pseudopod projection and cell spreading of passive leukocytes in response to fluid shear stress. *Biophys. J.* 87:2035–2042. http://dx.doi.org/10.1529/biophysj.104.042192

Eisa-Beygi, S., and X.Y. Wen. 2015. Could pharmacological curtailment of the RhoA/Rho-kinase pathway reverse the endothelial barrier dysfunction associated with Ebola virus infection?. *Antiviral Res.* 114:53–56. http://dx.doi.org/10.1016/j.antiviral.2014.12.005

Fujishiro, S.H., S. Tanimura, S. Mure, Y. Kashimoto, K. Watanabe, and M. Kohno. 2008. ERK1/2 phosphorylate GEF-H1 to enhance its guanine nucleotide exchange activity toward RhoA. *Biochem. Biophys. Res. Commun.* 368:162–167. http://dx.doi.org/10.1016/j.bbrc.2008.01.066

Galbraith, C.G., R. Skalak, and S. Chien. 1998. Shear stress induces spatial reorganization of the endothelial cell cytoskeleton. *Cell Motil. Cytoskeleton.* 40:317–330. http://dx.doi.org/10.1002/(SICI)1097-0169(1998)40:4<317::AID-CM1>3.0.CO;2-8

Green, C.E., D.N. Pearson, R.T. Camphausen, D.E. Staunton, and S.I. Simon. 2004. Shear-dependent capping of L-selectin and P-selectin glycoprotein ligand 1 by E-selectin signals activation of high-avidity beta2-integrin on neutrophils. *J. Immunol.* 172:7780–7790. http://dx.doi.org/10.4049/jimmunol.172.12.7780

Guilluy, C., V. Swaminathan, R. Garcia-Mata, E.T. O'Brien, R. Superfine, and K. Burridge. 2011. The Rho GEFs LARG and GEF-H1 regulate the mechanical response to force on integrins. *Nat. Cell Biol.* 13:722–727. http://dx.doi.org/10.1038/ncb2254

Heasman, S.J., L.M. Carlin, S. Cox, T. Ng, and A.J. Ridley. 2010. Coordinated RhoA signaling at the leading edge and uropod is required for T cell transendothelial migration. *J. Cell Biol.* 190:553–563. http://dx.doi.org/10.1083/jcb.201002067

Heck, J.N., S.M. Ponik, M.G. Garcia-Mendoza, C.A. Pehlke, D.R. Inman, K.W. Eliceiri, and P.J. Keely. 2012. Microtubules regulate GEF-H1 in response to extracellular matrix stiffness. *Mol. Biol. Cell.* 23:2583–2592. http://dx.doi.org/10.1091/mbc.E11-10-0876

Hyduk, S.J., J.R. Chan, S.T. Duffy, M. Chen, M.D. Peterson, T.K. Waddell, G.C. Digby, K. Szaszi, A. Kapus, and M.I. Cybulsky. 2007. Phospholipase C, calcium, and calmodulin are critical for alpha4beta1 integrin affinity up-regulation and monocyte arrest triggered by chemoattractants. *Blood.* 109:176–184. http://dx.doi.org/10.1182/blood-2006-01-029199

Ji, J.Y., H. Jing, and S.L. Diamond. 2008. Hemodynamic regulation of inflammation at the endothelial-neutrophil interface. *Ann. Biomed. Eng.* 36:586–595. http://dx.doi.org/10.1007/s10439-008-9465-4

Kakiashvili, E., P. Speight, F. Waheed, R. Seth, M. Lodyga, S. Tanimura, M. Kohno, O.D. Rotstein, A. Kapus, and K. Szászi. 2009. GEF-H1 mediates tumor necrosis factor-alpha-induced Rho activation and myosin phosphorylation: role in the regulation of tubular paracellular permeability. *J. Biol. Chem.* 284:11454–11466. http://dx.doi.org/10.1074/jbc.M805933200

Kitayama, J., A. Hidemura, H. Saito, and H. Nagawa. 2000. Shear stress affects migration behavior of polymorphonuclear cells arrested on endothelium. *Cell. Immunol.* 203:39–46. http://dx.doi.org/10.1006/cimm.2000.1671

Krendel, M., F.T. Zenke, and G.M. Bokoch. 2002. Nucleotide exchange factor GEF-H1 mediates cross-talk between microtubules and the actin cytoskeleton. *Nat. Cell Biol.* 4:294–301. http://dx.doi.org/10.1038/ncb773

Kuo, J.C., X. Han, C.T. Hsiao, J.R. Yates III, and C.M. Waterman. 2011. Analysis of the myosin-II-responsive focal adhesion proteome reveals a role for β-Pix in negative regulation of focal adhesion maturation. *Nat. Cell Biol.* 13:383–393. http://dx.doi.org/10.1038/ncb2216

Lämmermann, T., B.L. Bader, S.J. Monkley, T. Worbs, R. Wedlich-Söldner, K. Hirsch, M. Keller, R. Förster, D.R. Critchley, R. Fässler, and M. Sixt. 2008. Rapid leukocyte migration by integrin-independent flowing and squeezing. *Nature.* 453:51–55. http://dx.doi.org/10.1038/nature06887

Laudanna, C., J.J. Campbell, and E.C. Butcher. 1996. Role of Rho in chemoattractant-activated leukocyte adhesion through integrins. *Science.* 271:981–983. http://dx.doi.org/10.1126/science.271.5251.981

Lerman, Y.V., K. Lim, Y.M. Hyun, K.L. Falkner, H. Yang, A.P. Pietropaoli, A. Sonnenberg, P.P. Sarangi, and M. Kim. 2014. Sepsis lethality via exacerbated tissue infiltration and TLR-induced cytokine production by neutrophils is integrin α3β1-dependent. *Blood.* 124:3515–3523. http://dx.doi.org/10.1182/blood-2014-01-552943

Lowell, C.A., L. Fumagalli, and G. Berton. 1996. Deficiency of Src family kinases p59/61hck and p58c-fgr results in defective adhesion-dependent neutrophil functions. *J. Cell Biol.* 133:895–910. http://dx.doi.org/10.1083/jcb.133.4.895

Makino, A., E.R. Prossnitz, M. Bünemann, J.M. Wang, W. Yao, and G.W. Schmid-Schönbein. 2006. G protein-coupled receptors serve as mechanosensors for fluid shear stress in neutrophils. *Am. J. Physiol. Cell Physiol.* 290:C1633–C1639. http://dx.doi.org/10.1152/ajpcell.00576.2005

Mei, S.H., J.J. Haitsma, C.C. Dos Santos, Y. Deng, P.F. Lai, A.S. Slutsky, W.C. Liles, and D.J. Stewart. 2010. Mesenchymal stem cells reduce inflammation while enhancing bacterial clearance and improving survival in sepsis. *Am. J. Respir. Crit. Care Med.* 182:1047–1057. http://dx.doi.org/10.1164/rccm.201001-0010OC

Meiri, D., M.A. Greeve, A. Brunet, D. Finan, C.D. Wells, J. LaRose, and R. Rottapel. 2009. Modulation of Rho guanine exchange factor Lfc activity by protein kinase A-mediated phosphorylation. *Mol. Cell. Biol.* 29:5963–5973. http://dx.doi.org/10.1128/MCB.01268-08

Meiri, D., C.B. Marshall, M.A. Greeve, B. Kim, M. Balan, F. Suarez, C. Bakal, C. Wu, J. Larose, N. Fine, et al. 2012. Mechanistic insight into the microtubule and actin cytoskeleton coupling through dynein-dependent RhoGEF inhibition. *Mol. Cell.* 45:642–655. http://dx.doi.org/10.1016/j.molcel.2012.01.027

Meiri, D., C.B. Marshall, D. Mokady, J. LaRose, M. Mullin, A.C. Gingras, M. Ikura, and R. Rottapel. 2014. Mechanistic insight into GPCR-mediated activation of the microtubule-associated RhoA exchange factor GEF-H1. *Nat. Commun.* 5:4857. http://dx.doi.org/10.1038/ncomms5857

Nalbant, P., Y.C. Chang, J. Birkenfeld, Z.F. Chang, and G.M. Bokoch. 2009. Guanine nucleotide exchange factor-H1 regulates cell migration via localized activation of RhoA at the leading edge. *Mol. Biol. Cell.* 20:4070–4082. http://dx.doi.org/10.1091/mbc.E09-01-0041

Niggli, V. 2003a. Microtubule-disruption-induced and chemotactic-peptide-induced migration of human neutrophils: implications for differential sets of signalling pathways. *J. Cell Sci.* 116:813–822. http://dx.doi.org/10.1242/jcs.00306

Niggli, V. 2003b. Signaling to migration in neutrophils: importance of localized pathways. *Int. J. Biochem. Cell Biol.* 35:1619–1638. http://dx.doi.org/10.1016/S1357-2725(03)00144-4

Petri, B., J. Kaur, E.M. Long, H. Li, S.A. Parsons, S. Butz, M. Phillipson, D. Vestweber, K.D. Patel, S.M. Robbins, and P. Kubes. 2011. Endothelial LSP1 is involved in endothelial dome formation, minimizing vascular permeability changes during neutrophil transmigration in vivo. *Blood.* 117:942–952. http://dx.doi.org/10.1182/blood-2010-02-270561

Phillipson, M., B. Heit, S.A. Parsons, B. Petri, S.C. Mullaly, P. Colarusso, R.M. Gower, G. Neely, S.I. Simon, and P. Kubes. 2009. Vav1 is essential for mechanotactic crawling and migration of neutrophils out of the inflamed microvasculature. *J. Immunol.* 182:6870–6878. http://dx.doi.org/10.4049/jimmunol.0803414

Raftopoulou, M., and A. Hall. 2004. Cell migration: Rho GTPases lead the way. *Dev. Biol.* 265:23–32. http://dx.doi.org/10.1016/j.ydbio.2003.06.003

Ren, Y., R. Li, Y. Zheng, and H. Busch. 1998. Cloning and characterization of GEF-H1, a microtubule-associated guanine nucleotide exchange factor for Rac and Rho GTPases. *J. Biol. Chem.* 273:34954–34960. http://dx.doi.org/10.1074/jbc.273.52.34954

Rossy, J., D. Schlicht, B. Engelhardt, and V. Niggli. 2009. Flotillins interact with PSGL-1 in neutrophils and, upon stimulation, rapidly organize into membrane domains subsequently accumulating in the uropod. *PLoS One.* 4:e5403. http://dx.doi.org/10.1371/journal.pone.0005403

Smith, L.A., H. Aranda-Espinoza, J.B. Haun, M. Dembo, and D.A. Hammer. 2007. Neutrophil traction stresses are concentrated in the uropod during migration. *Biophys. J.* 92:L58–L60. http://dx.doi.org/10.1529/biophysj.106.102822

Springer, T.A. 1994. Traffic signals for lymphocyte recirculation and leukocyte emigration: the multistep paradigm. *Cell.* 76:301–314. http://dx.doi.org/10.1016/0092-8674(94)90337-9

Sumpio, B.E., S. Yun, A.C. Cordova, M. Haga, J. Zhang, Y. Koh, and J.A. Madri. 2005. MAPKs (ERK1/2, p38) and AKT can be phosphorylated by shear stress independently of platelet endothelial cell adhesion molecule-1 (CD31) in vascular endothelial cells. *J. Biol. Chem.* 280:11185–11191. http://dx.doi.org/10.1074/jbc.M414631200

Tsapara, A., P. Luthert, J. Greenwood, C.S. Hill, K. Matter, and M.S. Balda. 2010. The RhoA activator GEF-H1/Lfc is a transforming growth factor-beta target gene and effector that regulates alpha-smooth muscle actin expression and cell migration. *Mol. Biol. Cell.* 21:860–870. http://dx.doi.org/10.1091/mbc.E09-07-0567

Xu, J., F. Wang, A. Van Keymeulen, P. Herzmark, A. Straight, K. Kelly, Y. Takuwa, N. Sugimoto, T. Mitchison, and H.R. Bourne. 2003. Divergent signals and cytoskeletal assemblies regulate self-organizing polarity in neutrophils. *Cell.* 114:201–214. http://dx.doi.org/10.1016/S0092-8674(03)00555-5

Yamahashi, Y., Y. Saito, N. Murata-Kamiya, and M. Hatakeyama. 2011. Polarity-regulating kinase partitioning-defective 1b (PAR1b) phosphorylates guanine nucleotide exchange factor H1 (GEF-H1) to regulate RhoA-dependent actin cytoskeletal reorganization. *J. Biol. Chem.* 286:44576–44584. http://dx.doi.org/10.1074/jbc.M111.267021

Yuan, L., N. Sakamoto, G. Song, and M. Sato. 2013. Low-level shear stress induces human mesenchymal stem cell migration through the SDF-1/CXCR4 axis via MAPK signaling pathways. *Stem Cells Dev.* 22:2384–2393. http://dx.doi.org/10.1089/scd.2012.0717